[5] A. P. De Fonzo, C. H. Lee, and P. S. Mak, "Optically controllable millimeterwave phase shifter," *Appl. Phys. Lett.*, vol. 35, pp. 575–577, Oct. 1979.
[6] R. I. MacDonald and E. M. Hara, "Optoelectronic broadband switching array," *Electron. Lett.*, vol. 14, pp. 502–503, Aug. 1978.
[7] R. I. MacDonald and E. H. Hara, "Switching with photodiodes," *IEEE J. Quantum Electron.*, vol. QE-16, pp. 289–295, Mar. 1980.
[8] R. A. Kiehl and D. M. Drury, "An optically coupled microwave switch," in *1980 IEEE/MTT-S Intl. Microwave Symp. Dig.*, pp. 314–316, May 1980.
[9] H. Melchior and W. T. Lynch, "Signal and noise response of high-speed germanium avalanche photodiodes," *IEEE Trans. Electron Devices*, vol. ED-13, pp. 829–839, Dec. 1966.
[10] K. Stubjaer and M. Danielsen, "Nonlinearities of GaAlAs lasers harmonic distortion," *IEEE J. Quantum Electron.*, vol. QE-16, pp. 531–537, May 1980.
[11] K. Seki, M. Yano, T. Kamiya, and H. Yanai, "The phase shift of the light output in sinusoidally modulated semiconductor lasers," *IEEE J. Quantum Electron.*, vol. QE-15, pp. 791–797, Aug. 1979.
[12] M. R. Lakshminarayana, R. G. Hunsperger, and L. D. Partain, "Modulation of room-temperature GaAs lasers at *X*-band frequencies," *Electron. Lett.*, vol. 14, pp. 640–641, Sept. 1978.
[13] L. A. Glasser, "A linearized theory for the diode laser in an external cavity," *IEEE J. Quantum Electron.*, vol. QE-16, pp. 525–531, May 1980.
[14] F. K. Reinhart, "Efficient GaAs-$Al_xGa_{1-x}As$ double-heterostructure light modulators," *Appl. Phys. Lett.*, vol. 20, pp. 36–38, Jan. 1972.

✤

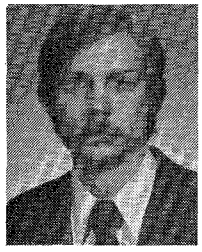

Richard A. Kiehl (M'75) was born in Akron, OH, on February 14, 1948. He received the B.S.E.E. (Honors Program) and M.S.E.E. degrees in 1970 and the Ph.D. degree in 1974 from Purdue University, West Lafayette, IN.

From 1971 to 1974 he was employed as a Research Assistant and Teaching Assistant in the School of Electrical Engineering, Purdue University. During that time he was engaged in research on transferred electron devices. From 1974 to 1980 he was a Member of Technical Staff at Sandia National Laboratories, Albuquerque, New Mexico, where his research was primarily focused on the study of various hybrid combinations of microwave and optical solid-state devices. Currently, he is a Member of Technical Staff at Bell Laboratories, Murray Hill, New Jersey, where he is engaged in the study of high-speed devices in compound semiconductors.

Dr. Kiehl is a member of Sigma Xi. He is a Past-Chairman of the Albuquerque Section of the IEEE.

✤

David M. Drury (S'76–M'78) was born in Casco, Wisconsin, on August 1, 1951. He received the B.S.E.E. degree from the Milwaukee School of Engineering, Milwaukee, WI, in 1972, the M.E.E. degree from the Midwest College of Engineering in 1975, and the Ph.D. degree in electrical engineering from Marquette University, Milwaukee, WI, in 1978.

From 1972 to 1976 he was a Development Engineer with Motorola Communications Division in Schaumburg, IL, and was engaged in the development of HF-SSB marine radios. Since 1978 he has been a Member of the Technical Staff of Sandia National Laboratories, Albuquerque, NM, engaged in exploratory radar development. His research interests include microwave and millimeter-wave solid state devices and circuits.

Dr. Drury is a member of Sigma Xi and is a registered Professional Engineer in Wisconsin.

Optoelectronic Microwave Switching via Laser-Induced Plasma Tapers in GaAs Microstrip Sections

WALTER PLATTE

Abstract—**This paper presents a new type of high-speed optoelectronic GaAs microstrip switch controlled by a pulse-operated laser diode via substrate-edge excitation. The exponential decay of photoconductivity across a longitudinal section of the microstrip forms a laser-induced electron-hole plasma wedge that works as a lossy tapered transmission line. The dynamics of carrier generation and recombination as well as the overall performance of the switch are quantitatively analyzed and optimized. This device is capable of switching with subnanosecond precision as well as with optical pulse energies in the order of 1 μJ. Theoretical and experimental results were found to be in good agreement.**

Manuscript received March 3, 1981; revised April 30, 1981. This work has been supported by Deutsche Forschungsgemeinschaft.

The author is with Institut fur Hochfrequenztechnik, Universitat Erlangen-Nuernberg, Cauerstr. 9, D-8520 Erlangen, West Germany.

I. Introduction

LASER-CONTROLLED solid-state microstrip switches (or optoelectronic switches) have gained much active interest within the last few years due to their picosecond

0018-9480/81/1000-1010$00.75 ©1981 IEEE

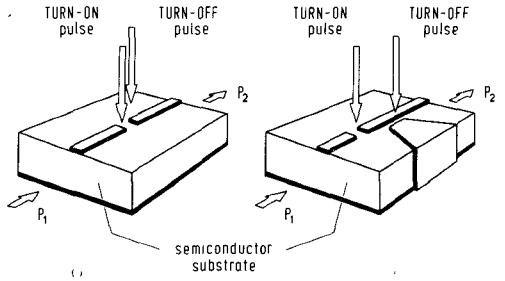

Fig. 1. Illustrations of optoelectronic microstrip switches with top-side excitation. (a) Single-gap structure, first used by Auston [1]. (b) Combined gap-shunt structure, first used by Platte [5].

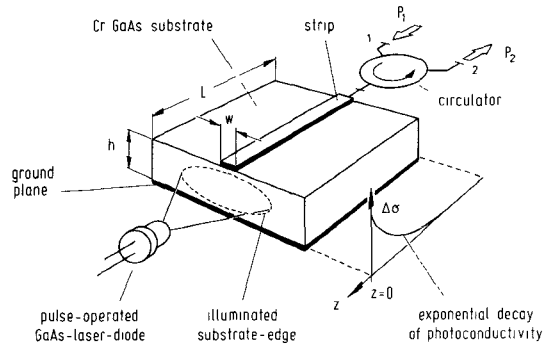

Fig. 2. Illustration of the GaAs switch with substrate-edge excitation.

precision, their simplicity of operation, and their inherently high isolation of electrical and optical signals. These devices can be successfully used for various applications such as the generation of ultrafast kilovolt pulses [1]–[3], high-speed microwave switching and controlling [4]–[7], high-frequency waveform generation [8], and picosecond high isolation sampling [9], [10].

Without considering the different substrate materials such as Si, GaAs, or InP, optoelectronic switches can be classified by the method of excitation. The first group includes devices with a single-gap structure (Fig. 1(a)), in which both the turn-on and the turn-off processes are achieved at the same location in the substrate [1], [2], [4], [7]–[9], [11], [12]. In this case, two optical pulses of greatly differing wavelengths are required to produce regions of highly conductive surface plasma and bulk plasma, respectively. If fast-recombination materials are used, e.g., Cr:GaAs [3], the device can turn off automatically due to the short lifetime of the excess carriers.

The second group includes optoelectronic switches with a combined gap-shunt microstrip structure (Fig. 1(b)) [5], [6], [10], [13], or with a coplanar gap structure [14], in which the turn-on and turn-off processes occur at different locations in the substrate. By this means, the controlling optical pulses may have the same wavelength, which offers the advantage of employing optical sources over a wide range of spectrum.

So far all types of optoelectronic switches have been controlled by focusing the laser pulses on a narrow gap or slot in the upper conductor of the microstrip as shown in Fig. 1 (top-side excitation). During the on-state of the switch the electrical signal is transmitted through a thin highly conductive plasma layer across the gap. During the off-state of the switch the transmission line is short-circuited by a second plasma region, preventing further transmission by totally reflecting the incident signal. Since the dimensions of the excited regions are usually much smaller than the signal wavelength, the overall performance of the switch can be calculated by lumped-element analysis [4], [6], [10], [12], [13]. In most cases of interest, the exponential decay of photoconductivity within the excited semiconductor region is of secondary importance.

In contrast to the above mentioned top-side excitation, this paper presents an alternative method of laser-controlled switching via substrate-edge excitation where the exponential decay of photoconductivity is the fundamental prerequisite for operation.

An open-ended GaAs microstrip section as shown in Fig. 2 is excited by laser pulses which are incident perpendicular to the microstrip cross section. If short-duration pulses are used and carrier diffusion may be neglected, a true exponential decay of carrier concentration as well as photoconductivity is produced along the z-axis of the microstrip. This specific distribution of the optically generated solid-state plasma between strip and ground plane may be considered as a laser-induced plasma wedge that works like a lossy tapered transmission line. During the on-state of the switch, i.e., if no optical excitation occurs, the electrical signal passes through the microstrip section without noticeable attenuation. It is then totally reflected at the open end of the microstrip and reenters the circulator after having passed through the microstrip section for the second time (return trip). During the off-state of the switch, i.e., if the laser-induced plasma taper is optimally activated, the incident microwave signal is totally absorbed within the excited substrate region, hence causing zero level at port 2 of the circulator. Owing to fast recombination in GaAs, the device returns automatically to its on-state. Unlike top-side excited switches, this device operates with inverted on- and off-states (i.e., optical pulse on turns switch off). This operation can be reversed if necessary by external circuitry such as bridge circuits, etc.

II. Analysis of Optoelectronic Performance

A. Laser-Pulse-Induced Photoconductivity

For the following quantitative analysis the GaAs substrate is assumed to have the typical properties of high-resistivity single-crystal material without any trapping effects, so that the applied laser pulses will cause a quasi-intrinsic electron-hole plasma with a nearly neutral excess carrier distribution, i.e., $\Delta n \approx \Delta p$. Neglecting carrier diffusion, surface recombination and surface charge effects, and supposing a nearly monochromatic radiation, the laser-pulse-induced photoconductivity $\Delta\sigma$ within the excited microstrip section (see Fig. 2) can be calculated from [13], [15]

$$\Delta\sigma(z) = \Delta\sigma_s \exp(\alpha_r z), \qquad z \leq 0 \tag{1a}$$

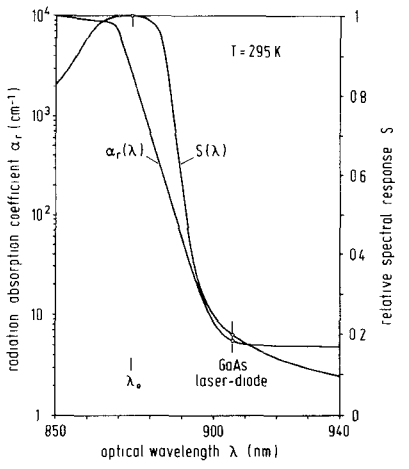

Fig. 3. Radiation absorption coefficient α_r [16], [17] and relative spectral response S [17] of bulk GaAs material as a function of optical wavelength λ.

with

$$\Delta\sigma_s=(q/2\pi\hbar c)(\mu_n+\mu_p)\alpha_r(\lambda)S(\lambda)(1-R_0)\eta_0\lambda_0\gamma_1 W/A \tag{1b}$$

where $\Delta\sigma_s$ is the surface photoconductivity at $z=0$, q is the electronic charge, $\hbar$ is the Planck's constant divided by 2π, c is the velocity of light in free space, μ_n and μ_p are the bulk mobilities of electrons and holes, $\alpha_r(\lambda)$ is the radiation absorption coefficient [16], [17], and $S(\lambda)$ is the relative spectral response of bulk Cr-doped GaAs [17] exhibiting a peak response at λ_0 (see Fig. 3). R_0 is the surface reflectivity and η_0 is the quantum yield of internal photoelectric effect, where the subscript 0 characterizes the values at λ_0. Bulk recombination effects are included in the factor $\gamma_1 \leqslant 1$ derived later in Section II-B. The variation or modulation of photoconductivity is generally indicated by the term W/A, i.e., the incident optical energy per unit area assuming a homogeneous power distribution across the illuminated substrate edge. Substituting in (1b) $(\mu_n+\mu_p)=4800$ cm^2/V·s, $R_0=0.32$, $\eta_0=1$, and $\lambda_0=0.874$ μm yields

$$\Delta\sigma_s=K\alpha_r(\lambda)S(\lambda)\gamma_1 W/A \tag{1c}$$

where $K=2.3\times10^{-3}$ cm$^2/\Omega\cdot\mu$J. When considering the problem of focusing the laser beam (Section IV) and the actual inhomogeneous distribution of irradiance across the laser spot, it is useful to introduce a correction factor $\gamma_2<1$ according to the following expression:

$$W/A=\gamma_2 W_p/wh \tag{2}$$

where w is the stripwidth, h is the substrate thickness, and W_p is the actual laser pulse energy which can be determined from a direct energy measurement with a calibrated detector or may be found approximately by using the well-known relation $W_p\approx P_p t_w$, i.e., the product of the radiant peak power P_p of the controlling pulses and the pulsewidth t_w. If the transversal power distribution of the controlling laser beam is given, e.g., as nearly Gaussian, it is well known that γ_2 can easily be calculated. When using laser diodes or arrays, however, the calculation or measurement of γ_2 is much more complicated and can only be carried out approximately (Section IV).

B. Influence of Excess Carrier Recombination

The switching operations of the device are internally controlled by carrier generation as well as by carrier recombination. These two physical mechanisms always work against each other. Their dynamics are found to dominate the performance of the switch [18] but cannot be separately analyzed, in general.

However, when employing optical pulses of pulsewidth $t_w \ll \tau$, where τ is the excess carrier lifetime of the substrate, carrier recombination may be neglected ($\gamma_1=1$) during the excitation phase ($0\leqslant t\leqslant 2t_w$), thus the rise of photoconductivity can be calculated as

$$\Delta\sigma_s(t)=(K\alpha_r S\gamma_2 P_p/wh)\int_0^t f(t)\,dt \tag{3}$$

where $f(t)$ is the pulse shape as a function of time. When using laser diodes or arrays, the pulses may be assumed to have a pure cosine shape (see Fig. 9(a)) according to

$$f(t)=0.5[1-\cos(\pi t/t_w)], \qquad 0\leqslant t\leqslant 2t_w \tag{4}$$

which can be considered as an excellent approximation [6]. Substituting (4) in (3) yields

$$\Delta\sigma_s(t)=(K\alpha_r S\gamma_2 W_p/2\pi wh)\cdot[(\pi t/t_w)-\sin(\pi t/t_w)], \qquad 0\leqslant t\leqslant 2t_w \tag{5}$$

where $W_p=P_p t_w$ and $\gamma_1=1$.

It can be seen from (5) that there is a time delay t_d between the peak value of photoconductivity and the peak value of the controlling optical pulse resulting in $t_d=t_w$ if $t_w \ll \tau$. During the recombination phase ($t\geqslant 2t_w$), the photoconductivity decreases exponentially with $\exp[(2t_w-t)/\tau)]$.

In the more general case, i.e., when applying optical pulses of pulsewidth $t_w \geqslant \tau$, the recombination is fast enough to diminish the optically generated electrons and holes almost instantaneously. This clearly will have a strong influence on the rise and peak value of photoconductivity. Assuming the excess carrier lifetime to be independent of excitation level, the buildup of the plasma taper can easily be calculated by studying the dynamics of the electrical equivalent circuit. This circuit consists of a capacitor (C) shunted by a resistor (R). C is charged by the load-independent current pulse $I(t)=I_p f(t)$ causing the voltage $U(t)$ across C. Consequently, the following pairs of analogous parameters may be set up: $C\rightarrow 1$, $R\rightarrow\tau$, $I_p\rightarrow P_p$, and $U(t)\rightarrow W(t)$. By this means, the photoconductivity can be expressed as

$$\Delta\sigma_s(t)=M\{1-\cos(\pi t/t_w)-(\pi\tau/t_w)\sin(\pi t/t_w)+(\pi\tau/t_w)^2[1-\exp(-t/\tau)]\}, \qquad 0\leqslant t\leqslant 2t_w \tag{6a}$$

and

$$\Delta\sigma_s(t)=M(\pi\tau/t_w)^2\exp(-t/\tau)\cdot[\exp(2t_w/\tau)-1], \qquad 2t_w\leqslant t\leqslant\infty \tag{6b}$$

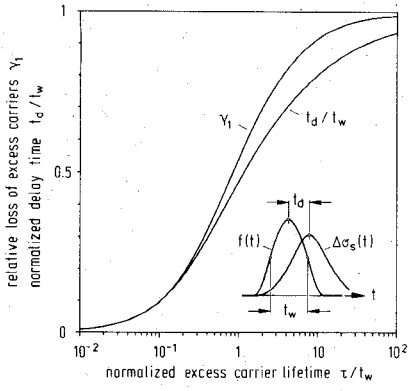

Fig. 4. Plot of normalized delay time t_d/t_w and relative loss of excess carriers γ_1 as a function of normalized excess carrier lifetime τ/t_w.

where

$$M=K\alpha_r S\gamma_2 W_p\tau/2wht_w\left[1+(\pi\tau/t_w)^2\right].$$

Now, t_d as well as γ_1 is a function of τ, which can easily be analyzed from (6a). The corresponding results are plotted in Fig. 4 and are clearly independent of f and W_p.

Finally, in the case of fast recombination where $\tau/t_w \ll 1$, (6) reduces to the simplified expression

$$\Delta\sigma_s(t)\approx\left[K\alpha_r S\gamma_2 W_p/wh\right] f(t)\tau/t_w \tag{7}$$

exhibiting a pulsed photoconductivity that is proportional to the optical pulse and follows it quasi-synchronously. The total loss of excess carriers is indicated by $\gamma_1=\tau/t_w$ corresponding to a net pulse energy $\gamma_1 W_p=P_p\tau$.

III. Analysis of Microwave Performance

A. Wave Propagation on Lossy Tapered Microstrip

When approximating the truly exponential decay of photoconductivity by a stepped multisection distribution of stepwidth Δz and conductivity ratio $m=\Delta\sigma_{\nu+1}/\Delta\sigma_\nu$ both being constant (Fig. 5, $m>1$), then the relative power reflection from a single step is given by

$$|\Gamma_\nu|^2=\left|\frac{Z_{\nu+1}-Z_\nu}{Z_{\nu+1}+Z_\nu}\right|=\frac{D_\nu+D_{\nu+1}-\delta}{D_\nu+D_{\nu+1}+\delta} \tag{8}$$

where

$$\delta=\left[(D_\nu+1)(D_{\nu+1}+1)\right]^{1/2}+\left[(D_\nu-1)(D_{\nu+1}-1)\right]^{1/2}$$

$$D_\nu=\left(1+\vartheta_\nu^2\right)^{1/2}\quad D_{\nu+1}=\left(1+m^2\vartheta_\nu^2\right)^{1/2}$$

$$Z_\nu=Z_l(1-j\vartheta_\nu)^{-1/2}$$

$$\vartheta_\nu=\Delta\sigma_\nu/\epsilon_0\epsilon_r\omega.$$

Z_ν is the characteristic impedance of the excited microstrip section ν with the substrate conductivity $\Delta\sigma_\nu$ being constant, Z_l is the characteristic impedance of a lossless microstrip line [19], ϑ_ν is the ' excitation loss tangent ' due to the induced photoconductivity. ϵ_0 is the free space permittivity, ϵ_r is the relative permittivity of the substrate, and ω is the angular frequency of the incident electrical signal. Since conductor losses, dielectric losses and dark-conductivity losses have been found to be of secondary importance for the relevant dynamics of the switch, these dark-substrate losses may be neglected in the following analysis.

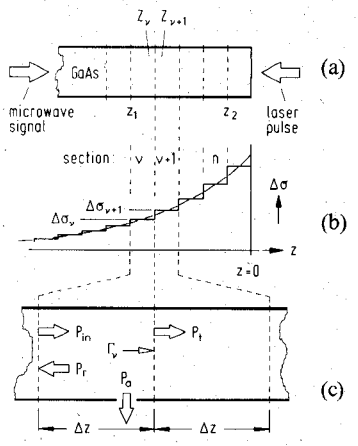

Fig. 5. Specific details for the analysis. (a) Longitudinal section of the excited microstrip region. (b) Exponential decay of photoconductivity and its approximation. (c) Power distribution in a single section.

In the case of an inhomogeneously excited microstrip transmission line as shown in Fig. 5, i.e., a lossy tapered transmission line, the major portion of losses is caused by the dominance of shunt conductance per unit length (G'), at least within the high-excitation region near $z=0$, resulting in $R'/\omega L'\ll 1$ and $G'/\omega C'\gg 1$, where R', G', L', and C' are the commonly used line parameters per unit length. Hence, the propagation constant γ may be expressed by

$$\gamma=\alpha+j\beta=\left[-(1-j\vartheta)\mu_0\mu_r\epsilon_0\epsilon_{re}\omega^2\right]^{1/2}$$

$$=\left\{\left[(1+\vartheta^2)^{1/2}-1\right]^{1/2}+j\left[(1+\vartheta^2)^{1/2}+1\right]^{1/2}\right\}\beta_l/\sqrt{2} \tag{9}$$

with

$$\beta_l=\left[\omega^2\mu_0\mu_r\epsilon_0\epsilon_{re}\right]^{1/2}$$

where α is the attenuation constant and β is the phase constant, β_l is the phase constant of a lossless microstrip line, μ_0 and μ_r are the free space and relative permeabilities, respectively, ϵ_{re} is the effective dielectric constant of the microstrip and $\vartheta=\Delta\sigma/\epsilon_0\epsilon_r\omega=G'/\omega C'$ assuming a uniform substrate excitation within any cross-sectional plane being parallel to the illuminated substrate edge.

If we neglect all multiple reflections between the individual differential sections, the power balance for a single section ν (Fig. 5(c)) is given by the following terms:
relative return power

$$p_r=P_r/P_{\text{in}}=|\Gamma_\nu|^2\exp(-4\alpha_\nu\Delta z) \tag{10}$$

relative transmitted power

$$p_t=P_t/P_{\text{in}}=\left(1-|\Gamma_\nu|^2\right)\exp(-2\alpha_\nu\Delta z) \tag{11}$$

relative absorbed power

$$p_a=P_a/P_{\text{in}}=1-p_r-p_t \tag{12}$$

where P_{in} is the reference input power and $\alpha_\nu=\alpha(\Delta\sigma_\nu)$.

The total distribution of p_r, p_t, and p_a per stepwidth Δz as a function of z along the plasma taper has been obtained

via computer analysis by taking the relative output power p_t of section ν as the relative input power of the following section $\nu+1$, and so on. This method yields a triple set of curves of discrete values for $p_r(z)$, $p_t(z)$, and $p_a(z)$. A successive reduction of stepwidth finally results in curves which agree excellently with the analytical results reported later in Section III-B.

The most important result of this computer analysis is the fact that p_r of any individual section vanishes as Δz approaches zero, independently of $\Delta\sigma$. This effect can be verified analytically from (8) by using the relationship between m and Δz in the case of an exponential decay of photoconductivity, i.e., $m=1+\alpha_r\Delta z$, which finally yields

$$|\Gamma_\nu|\approx\alpha_r\Delta z\left[\vartheta_\nu^2/4\left(1+\vartheta_\nu^2\right)\right], \qquad \text{if } \alpha_r\Delta z\ll 1. \tag{13}$$

From this, one obtains $|\Gamma_\nu|\to 0$ if $\Delta z\to 0$, which is found to be valid everywhere along the taper. Accordingly, the incident microwave signal is attenuated continuously in a smooth fashion without any reflections when propagating along the exponential plasma taper.

B. Overall Transmission and Absorption of Signal Power

After having found the incident microwave signal propagating along the plasma taper without any reflections, the total attenuation A and the total phase shift B across a finite taper length $d=z_2-z_1$ can be calculated analytically by summing up all the individual contributions obtained from (9) according to

$$A=\int_{z_1}^{z_2}\alpha(z)\,dz \tag{14}$$

and

$$B=\int_{z_1}^{z_2}\beta(z)\,dz \tag{15}$$

where $-\infty\leqslant z_1\leqslant z\leqslant z_2\leqslant 0$.

Letting $z_1\to-\infty$ and $z_2\to z$, the relative transmitted power (of an incident wave propagating in the positive z-direction) as a function of z is given by

$$p_t(z)^+=\exp\left[-2\int_{-\infty}^{z}\alpha(z)\,dz\right]$$
$$=\exp\left[-\frac{2\sqrt{2}}{\alpha_r}\beta_l\left\{a(z)-\frac{1}{\sqrt{2}}\tan^{-1}\frac{a(z)}{\sqrt{2}}\right\}\right], \qquad -\infty\leqslant z\leqslant 0 \tag{16a}$$

with

$$a(z)=\left\{\left[1+\vartheta^2(z)\right]^{1/2}-1\right\}^{1/2}$$

where $\vartheta(z)=\vartheta_s\exp(\alpha_r z)$ and $\vartheta_s=\Delta\sigma_s/\epsilon_0\epsilon_r\omega$, assuming that the microwave signal is totally absorbed before reaching the open end of the microstrip (see Fig. 6(b)).

If the signal is not totally absorbed (Fig. 6(a)), then it will be reflected at $z=0$ and will propagate back to the input. In this case, letting $z_1\to z$ and $z_2\to 0$, the corresponding power transmission in the negative z-direction can be calculated from

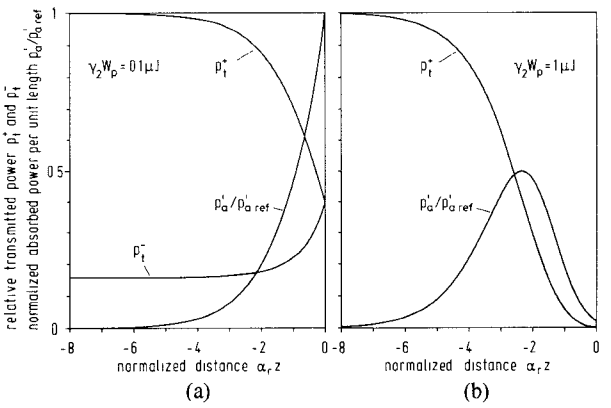

Fig. 6. Plot of relative transmitted power p_t^+ and p_t^- as well as normalized absorbed power per unit length $p_a'/p_{a\,ref}'$ against normalized distance $\alpha_r z$ in the case of: (a) $\gamma_2 W_p=0.1$ μJ; and (b) $\gamma_2 W_p=1$ μJ. ($\alpha_r=5.55$ cm^{-1}, $S=0.2$, $\gamma_1=1$, $h=0.08$ cm, $w=0.05$ cm, $f=8$ GHz, $\varepsilon_r=12.9$, $\varepsilon_{re}=8.4$, $\mu_r=1$, $p_{a\,ref}'=3.8$.)

$$p_t(z)^-=p_t(0)^+\exp\left[-2\int_z^0\alpha(z)\,dz\right]$$
$$=\exp\left[-\frac{2\sqrt{2}}{\alpha_r}\beta_l\left\{2a_0-a(z)-\sqrt{2}\tan^{-1}\frac{a_0}{\sqrt{2}}+\frac{1}{\sqrt{2}}\tan^{-1}\frac{a(z)}{\sqrt{2}}\right\}\right], \qquad -\infty\leqslant z\leqslant 0 \tag{16b}$$

where

$$a_0=a(z=0)=\left\{\left[1+\vartheta_s^2\right]^{1/2}-1\right\}^{1/2}.$$

If the switch is operated with microwave signals having power levels in the range of 500 mW or more (which clearly must all be dissipated within the excited semiconductor region), the substrate should be mounted on a heat sink preventing further signal absorption due to a thermally increased substrate conductivity during the on-state of the switch. For this case, it is useful to study the relative absorbed power per unit length $p_a'(z)$ as a function of z.

Referring to the stepped multisection distribution of $\Delta\sigma$ (Fig. 5(b)), the relative signal power $p_a(z_2)$ being absorbed in the differential section n may be expressed by

$$p_a(z_2)=P_a(z_2)/P_{\text{in}}(z_1)$$
$$=\left[1-\exp\left(-2\alpha_n\Delta z\right)\right]\cdot\exp\left(-2\sum_{\nu=1}^{n-1}\alpha_\nu\Delta z\right). \tag{17}$$

Allowing Δz to become infinitesimally small, i.e., $\Delta z\to dz$, (17) becomes

$$p_a(z_2)=2\alpha(z_2)\,dz\exp\left(-2\int_{z_1}^{z_2}\alpha(z)\,dz\right) \tag{18}$$

and hence, the relative absorbed power per unit length as a

function of z can be obtained from

$$p_a'(z)^+ = \sqrt{2}\beta_l a(z) p_t(z)^+, \qquad -\infty \leq z \leq 0 \quad (19a)$$

$$p_a'(z)^- = \sqrt{2}\beta_l a(z) p_t(z)^-, \qquad -\infty \leq z \leq 0 \quad (19b)$$

yielding in total

$$p_a'(z) = p_a'(z)^+ + p_a'(z)^-. \quad (19c)$$

Some typical shapes of $p_t(z)^+$, $p_t(z)^-$, and $p_a'(z)$ along with two different excitation levels are shown in Fig. 6. In the case of low excitation (Fig. 6(a)), the incident signal is continuously attenuated during its round trip through the plasma taper without being totally absorbed ($p_t^-(-\infty) > 0$). An effective power dissipation is obtained within the normalized distance $\alpha_r z \approx 6$ which corresponds to an effective taper length $l = 1.1$ cm. The maximum power dissipation occurs at $z = 0$.

When using sufficiently high excitation levels (Fig. 6(b)), the incident signal is totally absorbed ($p_t^+(0) = 0$) before being reflected at $z = 0$. The effective taper length is nearly 1.5 cm ($\alpha_r z \approx 8$). In this case, the region of maximum power dissipation is located at a depth of 0.4 cm ($\alpha_r z = 2.3$) below the illuminated substrate edge. Although the photoconductivity has been increased, the peak of $p_a'(z)$ is lower than that of the low-excitation taper.

Moreover, it should be noted, that the signal wavelength λ_m on the excited microstrip section is a function of z due to the locally varying phase constant $\beta(z)$. In the high-excitation region where $\vartheta \gg 1$, λ_m decreases exponentially as z increases according to the following expression:

$$\lambda_m(z) \approx (4\pi\epsilon_r/\epsilon_{re}\mu_0\mu_r f\Delta\sigma_s)^{1/2} \cdot \exp(-0.5\alpha_r z), \qquad -\infty \leq z \leq 0. \quad (20)$$

In general, this relationship ensures excellently matched plasma tapers having an effective taper length $l \gg \lambda_m$.

C. Inherent Propagation Delay

When studying in detail the propagation of an incident optical pulse as well as the propagation of an incoming microwave signal through a semiconductor substrate having ultrafast carrier recombination ($t_d \leq 1$ ps), it is seen that the switch response to the optical pulse appears with an inherent time delay t_i. This delay becomes minimal if, for example, picosecond laser pulses are used along with a wavelength that ensures strong optical absorption in the substrate. In this case, the incident laser pulse is totally absorbed within a thin surface layer below the illuminated substrate edge preventing further pulse propagation in the negative z-direction. Nevertheless, a small portion of the incoming microwave signal is absorbed by the thin plasma layer so that a somewhat reduced microwave signal propagates along the dark-substrate microstrip in the negative z-direction. Assuming that signal detection and recording are accomplished at $z = -L$ where L is the actual length of the microstrip (Fig. 2), the minimum propagation delay can be obtained from $t_{i\,\min} = L(\mu_0\mu_r\epsilon_0\epsilon_{re})^{1/2}$ yielding $t_{i\,\min} = 245$ ps if $\mu_r = 1$, $\epsilon_{re} = 8.4$, and $L = 2.54$ cm.

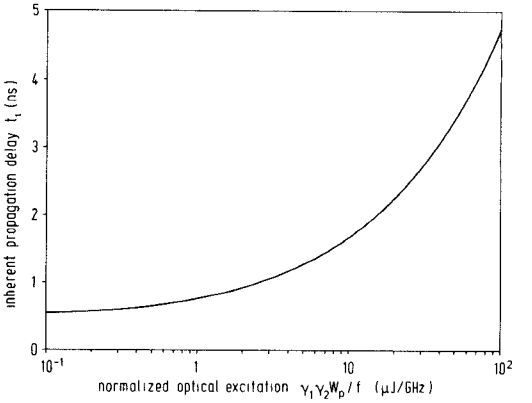

Fig. 7. Plot of inherent propagation delay t_i as a function of normalized excitation $\gamma_1\gamma_2 W_p/f$. ($Z_l = 50\ \Omega$, $h = 0.08$ cm, $w = 0.05$ cm, $L = 2.54$ cm, $\epsilon_{re} = 8.4$, $\mu_r = 1$, $\alpha_r = 5.55\ \text{cm}^{-1}$, $S = 0.2$.)

On the other hand, when employing laser pulses of pulsewidth $t_w \gg t_p$ where t_p is the time required by the laser pulse to propagate from $z = 0$ to $z = -L$ (e.g., $t_p = 305$ ps in GaAs if $L = 2.54$ cm) and assuming low optical absorption, the buildup of the plasma taper to its full effective length may be considered to be instantaneous. In this case, the signal propagation on the excited microstrip section is characterized by a locally varying phase velocity $v_p(z)$ which decreases as z increases. The delay between the peak of the detected microwave signal and the peak of the optical pulse then may be calculated from the following expression:

$$t_i = (L-l)(\mu_0\mu_r\epsilon_0\epsilon_{re})^{1/2} + 2\int_{z=-L}^{0} \frac{dz}{v_p(z)} l \quad (21)$$

where l is the effective taper length, e.g., $l = 1.1$ cm as estimated from Fig. 6(a).

However, since the physical determination of the actual effective taper length is impractical and prone to large experimental error, it is more useful to estimate the propagation delay from its upper limit where $l = L$, i.e., when the plasma taper extends over the full substrate length. Using the results obtained in Sections III-A and III-B, the propagation delay then may be calculated as

$$t_i = \frac{2}{\omega}\int_{z=-L}^{0} \beta(z)\, dz = (2\mu_0\mu_r\epsilon_0\epsilon_{re})^{1/2} \int_{z=-L}^{0} b(z)\, dz \quad (22)$$

where

$$b(z) = \left\{\left[1+\vartheta^2(z)\right]^{1/2} + 1\right\}^{1/2}$$

and further, after integration

$$t_i = \frac{(8\mu_0\mu_r\epsilon_0\epsilon_{re})^{1/2}}{\alpha_r} \cdot \left\{ b_2 - b_1 + \frac{1}{2\sqrt{2}} \ln\left[\frac{(b_2-\sqrt{2})(b_1+\sqrt{2})}{(b_2+\sqrt{2})(b_1-\sqrt{2})} \right] \right\} \quad (23)$$

where $b_1 = b(z=-L)$ and $b_2 = b(z=0)$. If $\vartheta_s = 0$, one obtains $b_1 = b_2 = \sqrt{2}$, and hence $t_i = 2t_{i\,\min}$. Fig. 7 shows a plot

of t_t as a function of $\gamma_1\gamma_2 W_p/f$ calculated from (23).

In general, dropping the restrictive condition of ultrafast carrier recombination, the total time delay between the switched output signal and the controlling laser pulse is clearly governed by both the propagation delay (t_t) as well as the delay caused by the optical generation of the plasma conductivity (t_d). In most cases of interest, this total delay has been found to be given approximately by the sum of t_t and t_d, especially in the case of $t_w \gg t_p$, $t_w \gg t_t$, and, of course, $t_w \gg 1/f$, which is applicable to the experimental conditions described in Section IV.

D. Optimum Switch Performance

Considering that the actual effective region of the plasma taper extends typically 10 to 100 optical penetration depths (which clearly depends on laser wavelength and excitation level) and furthermore, assuming that this effective taper length is smaller than the total length of the microstrip used, the input reflection coefficient Γ_m of the microstrip is approximately given by

$$\Gamma_m = \Gamma_0 \exp\left[-2\int_{-\infty}^{0} \alpha(z)\,dz - j2\int_{-\infty}^{0} \beta(z)\,dz\right] \quad (24)$$

where Γ_0 is the reflection coefficient of the open-ended microstrip section at $z=0$. Hence, using s-parameter analysis and substituting $\Gamma_0 = 1$, the power transmission coefficient $|s_{21}|^2 = P_2/P_1$ of the complete switch (i.e., including the circulator as shown in Fig. 2) can be obtained from the following expression:

$$|s_{21}|^2 = |\Gamma_m|^2 = \exp\left[-\frac{4\sqrt{2}}{\alpha_r}\beta_l\left(a_0 - \frac{1}{\sqrt{2}}\tan^{-1}\frac{a_0}{\sqrt{2}}\right)\right] \quad (25)$$

assuming that the circulator is ideal. Of course, the same expression can be obtained from (16b) by letting $z \to -\infty$.

Referring to the results obtained in Section II, it can be seen from (25) that the overall performance of the switch strongly depends on the laser wavelength λ, the effective optical pulse energy $\gamma_1\gamma_2 W_p$ and the signal frequency $f = \omega/2\pi$. To ensure optimum switch performance, the actual values of these basic parameters must be optimally related to each other. This often results in a troublesome experimental procedure.

However, this procedure can be successfully simplified by using the optimum performance diagram shown in Fig. 8 which has been obtained from an extensive computer evaluation of (25). The plotted curves are based on a characteristic impedance (dark substrate) of $Z_l = 50\ \Omega$ as well as an on–off signal ration of 40 dB corresponding to $|s_{21}| = 0.01$.

It is seen that the optical pulse energy must be increased as the signal frequency is decreased with a fixed laser wavelength, as expected. In the lower wavelength region (850–900 nm) the optical pulse energy decreases monotonically with increase of laser wavelength for a given signal frequency. This may be explained by the fact that a long smooth plasma taper at 900 nm ($\alpha_r \approx 10\ \text{cm}^{-1}$) is more effective than a short steep one at 850 nm ($\alpha_r \approx 10^4\ \text{cm}^{-1}$). Further, having passed a minimum at about 900 nm, the optical pulse energy increases with increasing laser wavelength due to a nearly constant absorption coefficient along with a strong decrease in photosensitivity. The minimum optical pulse energy is obtained between 900 nm and 910 nm, which obviously demonstrates the excellent optoelectronic adaptation between the GaAs substrate and the GaAs laser array used in the experiments.

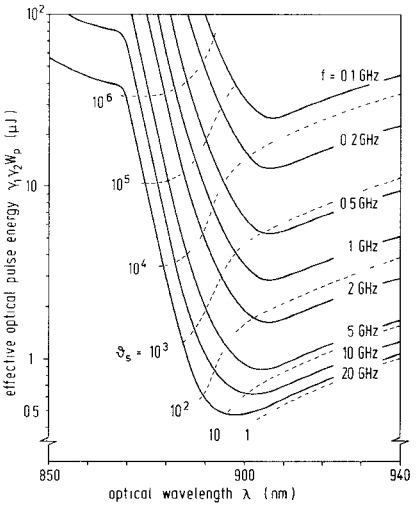

Fig. 8. Optimum performance diagram showing the effective optical pulse energy $\gamma_1\gamma_2 W_p$ required to produce $|s_{21}| = 0.01$ as a function of optical wavelength λ. The broken lines give the contours of constant excitation loss tangent. ($Z_l = 50\ \Omega$, $h = 0.08$ cm, $w = 0.05$ cm, $\varepsilon_r = 12.9$, $\varepsilon_{re} = 8.4$, $\mu_r = 1$, $|s_{21}| = 0.01$.)

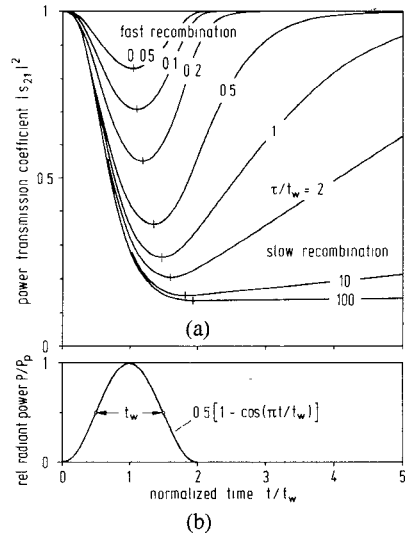

Fig. 9. Plot of the calculated switch response to a cosine optical pulse. (a) Controlling pure cosine pulse of radiant peak power P_p and pulsewidth t_w. (b) Calculated power transmission coefficient $|s_{21}|^2$ as a function of normalized time t/t_w with normalized excess carrier lifetime τ/t_w as parameter. ($\alpha_r = 5.55\ \text{cm}^{-1}$, $S = 0.2$, $h = 0.08$ cm, $w = 0.05$ cm, $\varepsilon_r = 12.9$, $\varepsilon_{re} = 8.4$, $\mu_r = 1$, $f = 1$ GHz, $\gamma_2 W_p = 0.2$ μJ, $t_t \ll t_d$.)

Finally, the relative output power $|s_{21}(t)|^2$ of the switch as a function of time can be calculated from (25) by substituting (6) in (25). Some typical envelopes (output signal after square-law detection) for the switch response to the controlling optical pulses are shown in Fig. 9 assuming

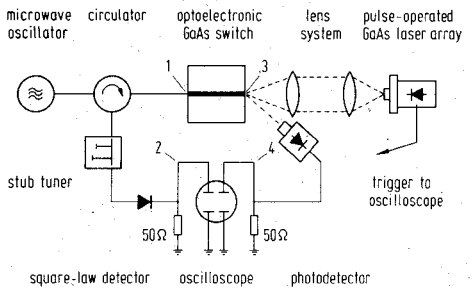

Fig. 10. Schematic of the experimental setup.

that $t_i \ll t_d$. These curves clearly show the strong influence of excess carrier recombination on the dynamic performance of the switch.

IV. Experimental Results

The results reported here are based on a 50-Ω microstrip transmission line ($w=0.05$ cm, $h=0.08$ cm, gold structures of 6-μm film thickness) fabricated on a Cr-doped GaAs substrate measuring 2.54 cm×2.54 cm×0.08 cm. The typical dark-substrate resistivity was 10^6 Ω·cm and the typical carrier lifetime was about 10^{-8} s. The device was controlled by cosine-like pulses of 90-ns pulsewidth and 100-Hz repetition rate which were generated from a GaAs laser array (RCA C 30009, four-strip type) radiating at 906 nm. The radiation emitted from the four array strips was focused rather weakly on the substrate edge to obtain the substrate-edge illumination as uniform as possible in the area where the field of an incoming microwave signal is mostly concentrated. The corresponding laser spot size detected via an image converter was found to be about 0.2 cm×0.08 cm yielding $\gamma_2 \approx 0.25$. Using the above-mentioned values of carrier lifetime and pulsewidth, the relative loss of excess carriers was found from Fig. 4 to be $\gamma_1 = 0.111$. Also the time delay due to optical carrier generation was obtained from Fig. 4 to be $t_d = 10$ ns. The maximum available radiant peak power actually incident on the substrate edge was measured with a calibrated detector resulting in $P_p =$ 54 W, and hence $\gamma_1\gamma_2 W_p = 0.135$ μJ.

Fig. 10 shows the experimental setup containing a signal path 1–2 used for the detection and recording of the switched microwave signal and a reference path 3–4 used for the detection and recording of the controlling laser pulses. Much care was taken to balance the external delay of each path, so that the specific time delay of the switch could be directly read from the oscilloscope. A typical pattern is shown in Fig. 11 where the upper trace monitors the switched and detected 1-GHz signal and the middle trace gives the zero-reference for the switched signal. The time delay between the switch response and the optical pulse monitored by the lower trace is about 12 ns which agrees fairly well with the theory: using $\gamma_1\gamma_2 W_p = 0.135$ μJ and $f=1$ GHz yields $t_i \approx 0.6$ ns (Fig. 7), and hence $(t_i + t_d) = 10.6$ ns. Furthermore, an increase in f and/or a decrease in W_p caused a small reduction of the total delay, which confirms experimentally the results obtained in Section III-C.

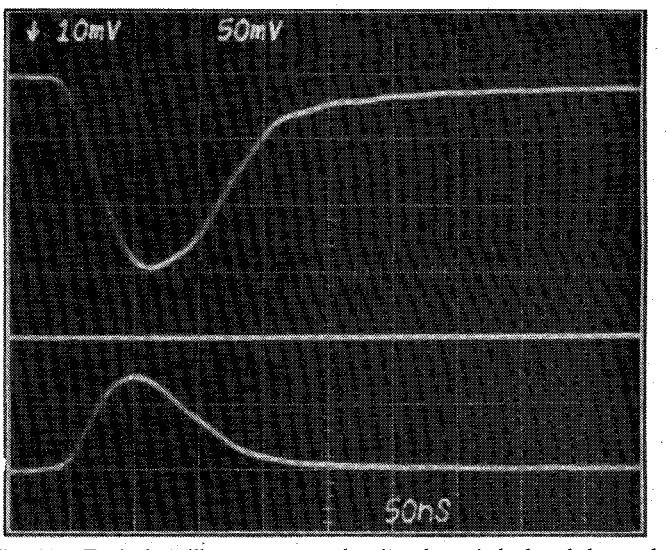

Fig. 11. Typical oscilloscope traces showing the switched and detected 1-GHz signal (upper trace), the zero-reference for the switched signal (middle trace), and the controlling 54-W laser pulse (lower trace).

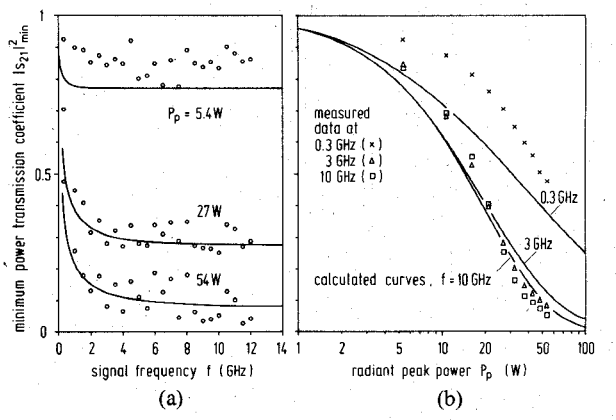

Fig. 12. The variation of minimum power transmission coefficient $|s_{21}|^2_{min}$ as: (a) a function of signal frequency f; and (b) a function of actually incident radiant peak power P_p. ($\alpha_r = 5.55$ cm^{-1}, $S=0.2$, $h=0.08$ cm, $w=0.05$ cm, $\mu_r=1$, $Z_l=50$ Ω, $\varepsilon_r=12.9$, $\varepsilon_{re}=8.4$, $t_w=90$ ns, $\tau=10$ ns, $\gamma_1=0.111$, $\gamma_2=0.25$.) Note that the measured data in (a) exhibit a quasi-periodicity due to the interference between the switched signal and the signal which leaks directly through the circulator.

To operate the RF detector in its square-law region the incident microwave power was kept sufficiently small. By this means, a vertical scale reading linearly proportional to $|s_{21}|^2$ was obtained, e.g., $|s_{21}|^2_{min} = 0.26$ from Fig. 11. The variation of $|s_{21}|^2_{min}$ as a function of the signal frequency f as well as of the actually incident radiant peak power P_p is recorded in Fig. 12.

V. Conclusions

A new type of high-speed optoelectronic microstrip switch on GaAs substrate using substrate-edge excitation has been presented. The dynamics of the switch and its overall performance have been studied theoretically as well as experimentally. The experimental results have been found to verify the theory fairly well considering that several of the parameter values involved in the theory may differ from the actual specimen values.

In comparison with top-side excited switches, this device can be operated at lower pulse intensities ranging from 0.5 to 5 μJ, which offers the advantage of employing small diode lasers for highly effective optoelectronic switching. Owing to the excellent optoelectronic adaptation between a Cr-doped GaAs substrate and a GaAs laser diode radiating near 900 nm, an integration of the switch and the controlling laser diode in a single substrate should be possible. This would open a wide range of new applications.

Although nanosecond laser pulses were used in these experiments (laser diodes producing shorter pulses were not available at the time these experiments were performed), the device is capable of switching with subnanosecond precision. For example, when employing picosecond pulses, the switch can successfully be used in the field of high-isolation sampling technique if the inherent propagation delay is kept sufficiently small and picosecond-recombination substrates are used. On the other hand, when employing CW-operated light emitting diodes, the device can work as a light-controlled matched or adjustable resistive load, which should allow interesting possibilities in the area of microstrip measurements. Corresponding investigations are currently in progress.

Acknowledgment

The author would like to thank Prof. H. Brand for his continuing encouragement and many helpful discussions. He also wishes to thank W. Renz for his technical assistance during the experiments as well as J. O. Schaefer for reading of this script.

References

[1] D. H. Auston, "Picosecond optoelectronic switching and gating in silicon," *Appl. Phys. Lett.*, vol. 26, pp. 101–103, 1975.
[2] P. Lefur and D. H. Auston, "A kilovolt picosecond optoelectronic switch and Pockels cell," *Appl. Phys. Lett.*, vol. 28, pp. 21–23, 1976.
[3] C. H. Lee, "Picosecond optoelectronic switching in GaAs," *Appl. Phys. Lett.*, vol. 30, pp. 84–86, 1977.
[4] A. M. Johnson and D. H. Auston, "Microwave switching by picosecond photoconductivity," *IEEE J. Quantum Electron.*, vol. QE-11, pp. 283–287, 1975.
[5] W. Platte, "High-speed optoelectronic switching in silicon gap-shunt microstrip structures," *Electron. Lett.*, vol. 12, pp. 437–438, 1976.
[6] W. Platte, "Pulse shaping by laser-excited solid-state plasmas in silicon," *Electron. Lett.*, vol. 12, pp. 631–633, 1976.
[7] C. H. Lee, S. Mak, and A. P. DeFonzo, "Millimeter-wave switching by optically generated plasma in silicon," *Electron. Lett.*, vol. 14, pp. 733–734, 1978.
[8] J. M. Proud and S. L. Norman, "High-frequency waveform generation using optoelectronic switching in silicon," *IEEE Trans. Microwave Theory Tech.*, vol. MTT-26, pp. 137–140, 1978.
[9] A. J. Low and J. E. Carroll, "10ps optoelectronic sampling system," *Inst. Elec. Eng. J. Solid-State Electron Devices*, vol. 2, pp. 185–190, 1978.
[10] W. Platte, "Optimum design and performance of optoelectronic sampling components on silicon substrate," *Electron. Commun.* (AEÜ), vol. 33, pp. 364–370, 1979.
[11] F. J. Leonberger and P. F. Moulton, "High-speed InP optoelectronic switch," *Appl. Phys. Lett.*, vol. 35, pp. 712–714, 1979.
[12] J. A. Buck, K. K. Li, and J. R. Whinnery, "Optoelectronic switching in a stub transmission line," *J. Appl. Phys.*, vol. 51, pp. 769–771, 1980.
[13] W. Platte, "Spectral dependence of microwave power transmission in laser-controlled solid-state microstrip switches," *Inst. Elec. Eng. J. Solid-State Electron Devices*, vol. 2, pp. 97–103, 1978.
[14] R. Castagne, S. Laval, and R. Laval, "Picosecond 1-wavelength optoelectronic gate," *Electron. Lett.*, vol. 12, pp. 438–439, 1976.
[15] A. Ambroziak, *Semiconductor Photoelectric Devices*. London: Iliffe, 1968, pp. 189–191.
[16] M. D. Sturge, "Optical absorption of Gallium Arsenide between 0.6 and 2.75 eV," *Phys. Rev.*, vol. 127, pp. 768–773, 1962.
[17] A. L. Lin and R. H. Bube, "Photoelectronic properties of high-resistivity GaAs:Cr," *J. Appl. Phys.*, vol. 47, pp. 1859–1867, 1976.
[18] W. Platte, "On the excitation-dependent decay of photoconductivity in laser-controlled solid-state switches," *Frequenz*, vol. 32, pp. 57–62, 1978.
[19] H. A. Wheeler, "Transmission-line properties of parallel strips separated by a dielectric sheet," *IEEE Trans. Microwave Theory Tech.*, vol. MTT-13, pp. 172–185, 1965.

Walter Platte was born in Remscheid, Germany, on January 24, 1943. He received the Dipl.-Ing. degree in electrical engineering from the Technical University of Aachen, Aachen, West Germany, in 1968, and the Dr.-Ing. degree in electrical engineering from the University of Erlangen-Nuernberg, Erlangen, West Germany, in 1975.

From 1968 to 1969, he worked at AEG-Telefunken, Ulm, West Germany, on the field of *Ku*-band radar instrumentation and measurement, especially on Doppler radar moving target simulators. Since October 1969, he has been with the Department of High-Frequency Techniques, University of Erlangen-Nuernberg, where he is engaged in the research of laser-controlled MIC components. In addition, he has been lecturing on light emitting and detecting devices at the University of Erlangen-Nuernberg since 1977.

Dr. Platte is member of the Verband Deutscher Elektrotechniker (VDE), and the Board of the Nachrichtentechnische Gesellschaft (NTG). In 1977, he received the NTG-Award for research and publications on high-speed optoelectronic microwave switching.